Improved Method for Permittivity Determination of Dielectric Samples by Free-Space Measurements

Ugur Cem Hasar, *Member, IEEE*, Yunus Kaya, Hamdullah Ozturk, Mucahit Izginli, Mehmet Ertugrul, *Member, IEEE*, Joaquim José Barroso, *Member, IEEE*, and Omar M. Ramahi, *Fellow, IEEE*

Abstract—A new deembedding technique is proposed for relative complex permittivity ε_r determination of dielectric materials using gated free-space measurements. Its three main features are 1) it does not require any formal calibration procedure (calibration-free); 2) it is position-insensitive; and 3) it extracts ripple-free ε_r due to gating process. The objective function derived to determine ε_r by the proposed method is validated by free-space measurements of three dielectric samples (polypropylene, polyethylene, and polyoxymethylene). Besides, the accuracy of our method is compared with the accuracy of other calibration-free and calibration-dependent methods in the literature.

Index Terms—Complex permittivity, deembedding technique, free-space, gating, uncalibrated measurements.

I. INTRODUCTION

MICROWAVE characterization and electromagnetic property extraction have been gaining more attention nowadays due to the attractive features of microwave signals, as compared with other techniques including ultrasound, optic spectroscopy, and chromatography, such as good penetration into nonmetallic structures, resistance to environmental conditions, and instantaneous measurement capability [1]. In recent years, microwave signals have been utilized in various applications ranging from super lens, invisibility cloak [2], 2-D metasurfaces [3], and examination of carbon fiber reinforced concrete structures [4] to adulteration detection within agricultural foods [5].

Microwave techniques used for characterization and electromagnetic property extraction can be categorized into two

groups as resonant techniques and nonresonant techniques [1]. Resonant techniques use specially designed measurement cells such as reentrant cavities, cylindrical and rectangular cavities, and open resonators to measure electromagnetic properties of samples [1], [6], [7]. The material characterization by resonant methods relies on measurement of a shift in resonance frequency and a change in quality factor after the sample is inserted into the cell. Although resonant techniques have better accuracy and resolution, they are band-limited and suffer from a careful sample preparation/machining process (much labor-intensive). More information about material and its frequency response, especially for newly designed materials, can be gained by measuring its internal electromagnetic response by nonresonant methods because, as their name implies, they are broadband and have relatively good accuracy. Material characterization by nonresonant techniques is implemented by way of measured reflection and transmission properties of the sample under analysis [1], [6], [7].

Nonresonant techniques can also be grouped into guided-line technique [8] and free-space technique [9]. While the former technique, in general, requires a guiding environment and contact between transmitter and receiver ends (e.g., metallic waveguide spacer/washer within which the sample is present for classical waveguide measurements), the latter technique is noncontacting and uses air as the energy transmission environment. Besides, while guided-line techniques requiring sample insertion become impractical at higher frequencies such as millimeter-wave and terahertz wave frequencies (very large wavelength), free-space techniques could be an attractive solution for such measurements [10]. In addition, free-space techniques are very useful for measurements at high temperatures due to no-physical contact between transmitter and receiver antennas [11]. Free-space measurement techniques can as well be classified as 1) reflection-type and 2) reflection/transmission-type [1], [10]. Materials can be characterized by Brewster angle and metal-backed-sample measurements for reflection-type free-space techniques. However, they have the ill-condition of determining the product of relative complex permittivity (ε_r) and relative complex permeability (μ_r). On the other hand, there are a variety of reflection/transmission-type free-space measurement configurations including, U-shape and Z-shape with/out polarizers, reflectors, and lenses [10]. These configurations supplement sufficient information for accurate

extraction of both ε_r and μ_r. For more information, the interested reader can refer to a recent review article for free-space techniques [10]. Our focus in this study is to apply reflection/transmission-type free-space microwave measurement techniques for extraction of electromagnetic property of solid planar materials.

Time-domain analysis [12]–[16] or frequency-domain analysis [4], [9], [11], [17]–[25] can be implemented in electromagnetic property extraction of materials by free-space techniques. Time-domain analysis uses temporal response of the sample from a signal source generated by a pulse generator, and then electromagnetic properties of the sample are determined by way of measurements of travel time within and attenuation across the sample. On the other hand, frequency-domain analysis utilizes a signal source operating over some frequency range to measure reflected signal from and transmitted signal through the sample, and thereafter electromagnetic properties of the sample by applying a suitable extraction algorithm. Different unique advantages and severe drawbacks of time-domain and frequency-domain analyses are present. For example, multipath signals or undesired signals from ground (or environment) can interfere with the main response of the sample (the response of the sample in the direction of line of sight between transmitting and receiving antennas) in free-space measurements, and the effect of these signals on the measured response of the sample can be removed or significantly eliminated by means of a time-domain gating process implemented directly by many modern vector network analyzers (VNAs) or realized by some signal processing techniques (a postmeasurement analysis) [22]. On the other hand, time-domain free-space techniques essentially assume that the frequency response of the sample is relatively constant (the sample is either nondispersive or weakly dispersive) in the extraction process of electromagnetic properties of the sample [15], [16]. However, in a real measurement scenario, the sample demonstrates some dispersive behavior over a broad frequency band and the abovementioned assumption is difficult to satisfy for broadband measurements.

Besides, a microwave measurement setup in general necessitates application of a suitable calibration process before (calibrated) measurements of the sample response are being carried out [4], [9], [11], [17]–[23]. There are various calibration techniques from highly accurate ones such as the short-open-load-thru (SOLT), thru-reflect-line (TRL) [26], thru-reflect-match (TRM) [27], and line-network-network (LNN) [28] to simple calibration techniques based on averaging (baseline measurement) technique [18], [29] or its variant forms [23]–[25]. Effects of any inaccurate calibration standard(s) used in the calibration procedure and/or improper implementation of calibration technique result in not only inaccurate description of the scattering (S-) matrix of the network, but also inappropriate deembedding (moving the measurement reference plane to the ends of the network). For instance, in implementation of the method in the study [24], the front face of the sample must be at the same place of the perfect electric conductor used in the process of calibration. In addition, the same stipulation is also required for the application of TRL, TRM, and LNN techniques in frequency-domain free-space measurements. Besides, it is expected that measurement accuracy of the techniques in the studies [4], [9], [11], [15], [17]–[23] will be higher than the measurement accuracy of the techniques [24], [25], because they utilize eight-term error network models in the analysis than simplified error network term(s) or model(s). It was assumed that the multiple-reflections within the sample were neglected, and the transmitting antenna was assumed to be reciprocal in the study [24]. In addition, simplified eight-term error network model (just one eight-term error network) was utilized in free-space measurements in the study [25].

Deembedding techniques relying on the eight-term error network model could be conveniently used to eliminate the aforementioned two effects (usage of inaccurate calibration standard(s) and misimplementation of the applied calibration technique) without resorting to determination of the error networks [30]–[41]. However, in some circumstances, they have the problem of producing some additional postprocess ripples. Sometimes, these techniques are coined as calibration-free techniques because they deemed eight-term error networks in electromagnetic characterization of samples. Refer to Section II-A for more details. In this study, we combine the advantages of time-domain and frequency-domain free-space techniques and propose a novel deembedding free-space technique using gated uncalibrated frequency-domain free-space measurements without necessitating any calibration procedure. In addition, another important advantage of the proposed technique is that, in contrast to the TRL and TRM calibration techniques, it does not necessitate the motion of the transmitting and receiving antennas throughout the material characterization process (precalibration and postcalibration measurements). Another important feature related to the previous advantage of the proposed method is that the proposed free-space technique is position-insensitive, meaning that there is no precise reference planes in the measurement process. Finally, our proposed method is similar (in terms of simplicity) to but has better accuracy than the free-space baseline technique [18], [29] or its variant forms [23]–[25], although they have similar measurement steps (line connection (empty air region) and sample connection), because our deembedding method evaluates ε_r without resorting to the determination of two-port error-networks represented by an eight-term error model [26].

II. METHOD

Fig. 1(a) and (b) display the schematic views of two measurement configurations for relative complex permittivity ε_r of a planar dielectric sample ($\mu_r = 1$ is the relative permittivity of the sample) with thickness L by our extraction technique. While Fig. 1(a) shows the measurement configuration when no sample is present between antennas, Fig. 1(b) illustrates the measurement configuration after the planar sample is positioned over arbitrary planes (plane-1 and plane-2) between antennas. Our technique determines ε_r of the sample using gated calibration-free S-parameter measurements.
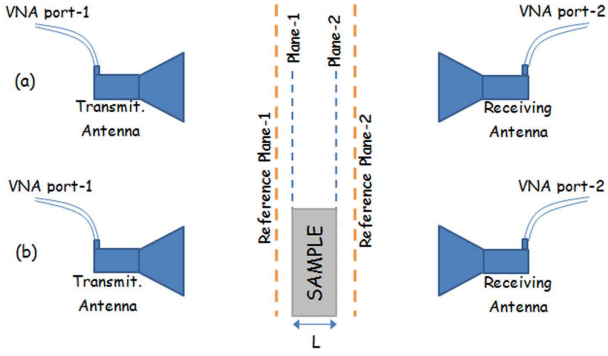
Fig. 1. Schematic views of the measurement configurations of the conventional deembedding method and the proposed deembedding method. (a) Line connection (no sample is present between plane-1 and plane-2). (b) Sample is positioned between plane-1 and plane-2. Here, reference plane-1 and reference plane-2 are considered as the planes over which the free-space measurements are assumed to be gated.

A. Conventional Deembedding Method

Assuming that the wave incident onto the sample is a plane wave, the wave-cascading matrices (WCMs) of both configurations in Fig. 1(a) and (b) (M_a and M_b) can be written as [31], [35]

$$M_k = \frac{1}{S_{21k}} \begin{bmatrix} S_{21k}S_{12k} - S_{11k}S_{22k}, & S_{11k} \\ -S_{22} & 1 \end{bmatrix} \quad (1)$$

$$M_a = T_X T_{S0} T_Y \quad (2)$$

$$M_b = T_X T_S T_Y. \quad (3)$$

Here, $k = a$ or b; S_{11k}, S_{21k}, S_{12k}, and S_{22k} are the forward and backward reflection and transmission S-parameters of the configurations in Fig. 1(a) and (b); T_X (T_Y) is the WCM of the eight-term error network [26] corresponding to the region between the port-1 (port-2) of VNA and the sample front (rear) face (transition changes, cable inhomogeneities, and VNA imperfection such as reflection/transmission frequency (tracking) errors, directivity, and source/load (port) mismatches [42]), and T_S and T_{S0} are the WCMs of the sample region and the air region with the same L. The expressions of T_S and T_{S0} are given as [30], [35], [37], [39]–[41]

$$T_S = \frac{1}{(1-\Gamma^2)T} \begin{bmatrix} (T^2 - \Gamma^2) & \Gamma(1 - T^2) \\ -\Gamma(1 - T^2) & 1 - \Gamma^2 T^2 \end{bmatrix} \quad (4)$$

$$T_{S0} = \begin{bmatrix} T_0 & 0 \\ 0 & 1/T_0 \end{bmatrix}, \quad T_0 = e^{-\gamma_0 L}, \quad \gamma_0 = j\frac{\omega}{c} \quad (5)$$

$$T = e^{-\gamma_0 n L}, \quad \Gamma = \frac{z-1}{z+1}, \quad z = \frac{1}{\sqrt{\varepsilon_r}}, \quad n = \sqrt{\varepsilon_r} \quad (6)$$

where T and T_0 are the propagation factors within the sample and air region with L; Γ is the interfacial reflection coefficient at the interface formed by air and the sample; n and z are the refractive index and the intrinsic (normalized wave) impedance of the sample; γ_0 is the propagation constant of air; ω is the angular frequency; and c is the velocity of light in vacuum (or approximately equal to that in air). Here, the time reference in the form $\exp(+j\omega t)$ is considered.

It is seen from (4) to (6) that T_S is a function of ε_r through the quantities z and T. Therefore, to determine ε_r using M_a

and M_b, the effects of unknown error networks T_X and T_Y must be eliminated from measured M_a and M_b. In this regard, the following two-step procedure is applied in the literature. First, the effect of the error network T_Y is eliminated by the multiplication of M_b with the inverse of M_a; that is,

$$M_b M_a^{-1} = T_X T_S T_{S0}^{-1} T_X^{-1}. \quad (7)$$

As a second step, the similarity between $M_b M_a^{-1}$ and $T_S T_{S0}^{-1}$ is exploited to remove the effect of the error network T_X in determination of ε_r as

$$\text{Tr}(M_b M_a^{-1}) = \text{Tr}(T_S T_{S0}^{-1}) \quad (8)$$

where $\text{Tr}(\star)$ denotes the trace operation of the square matrix "$\star$." Incorporating (4) and (5) into (8), one can derive the following objective function F_{obj} for ε_r evaluation [35]:

$$F_{\text{obj}}(\varepsilon_r) = \text{Tr}(M_b M_a^{-1}) - \frac{1}{(1-\Gamma^2)T}$$
$$\times \left[\frac{T^2 - \Gamma^2}{T_0} + T_0(1 - \Gamma^2 T^2) \right] = 0. \quad (9)$$

It is seen from (9) that ε_r can be evaluated by using any 2-D numerical technique such as the Newton's method or any optimization technique such as the "fminsearch" function of MATLAB, using initial guesses for ε_r provided with preliminary information in the literature.

B. New Deembedding Method

Extracted ε_r by the conventional deembedding calibration-free technique using F_{obj} in (9) could produce undesired ripples in ε_r over the whole frequency band [41]. To eliminate these ripples in the extraction process of ε_r by the proposed method, we use a variant form of the measurement configurations in Fig. 1 by considering two new planes (reference plane-1 and reference plane-2) over which time-gating is applied.

Considering the configurations in Fig. 1(a) and (b), it is possible to rewrite M_a and M_b in (2) and (3) as

$$M_a = T_X' T_{R1} T_{S0} T_{R2} T_Y' \quad (10)$$

$$M_b = T_X' T_{R1} T_S T_{R2} T_Y' \quad (11)$$

where T_X' (T_Y') denotes the error network corresponding to the region between the port-1 (port-2) of VNA and the reference plane-1 (plane-2) (transition changes, cable inhomogeneities, and VNA imperfection such as frequency error and source/load mismatches); and T_{R1} (T_{R2}) is the WCM of the air regions between reference plane-1 (plane-2) and plane-1 (plane-2).

It is seen from (2), (3), (10), and (11) that $T_X = T_X' T_{R1}$ and $T_Y = T_{R2} T_Y'$. Utilizing the procedures described in Section II-A (multiplying M_b with the inverse of M_a and applying the similarity matrix property to $M_b M_a^{-1}$ and $T_S T_{S0}^{-1}$), one can derive the same objective function in (9). It should be mentioned here that although different reference planes (see Fig. 1) are utilized for the analysis of conventional and new deembedding techniques, we still derive the same objection function. Besides, even though the same objective functions are to be utilized in the extraction process for the conventional and new deembedding techniques, the extracted ε_r will differ for both techniques because the time-gating

process, as validated by measurements in Section III, improves the accuracy of extraction process.

There are few important points related to our method. First, the proposed new deembedding calibration-free technique is similar to the conventional deembedding calibration-free technique [31], [35] discussed in Section II-A. However, our deembedding technique incorporates time-gating process into the evaluation of ε_r which significantly eliminates the ripples observed in the ε_r, to be demonstrated in Section III-B, by the conventional deembedding calibration-free technique [31], [35]. Here, this gating process allows to pick up only the useful reflected and transmitted signals (e.g., multiple reflections within the sample) and eliminate undesired reflected and transmitted signals (e.g., signals reflected from ground and between antennas) over some definitive time period. Second, the idea used in the new deembedding calibration-free technique is similar to the idea behind the gated-reflect-line (GRL) calibration technique [43], [44]. However, our proposed technique is a calibration-free technique while the GRL technique is a calibration technique meaning that S-parameter measurements of the sample must be performed after the GRL calibration technique. Third, on the contrary to the GRL technique, our calibration-free technique does not necessitate the use of any reflect standard with high reflectivity [only the S-parameter measurements through the air region between the reference plane-1 and the reference plane-2 in Fig. 1(a)] which may introduce calibration errors, especially for phase measurements, if the reflect standard has a substantial thickness and is not properly positioned at correct reference planes. Fourth, it is a position-insensitive method meaning that the sample can be located anywhere between the reference plane-1 and the reference plane-2, provided that the plane wave assumption is satisfied between these planes (sample is located in the far-field of from antennas). Fifth, it does not need the application of any calibration procedure before starting the application of time-gating process in free-space measurements as opposed to the case in the study [22]. Finally, the accuracy of our proposed formalism is much better than the classical baseline measurement techniques [18], [29] which use the normalization of (magnitude of) measured S_{21} (S_{11}) of the sample to that of the air (a highly reflective metal plate) for transmission (reflection) measurements (without considering eight-term error networks T_X and T_Y), because our method takes into account T_X and T_Y in the theoretical analysis [26]. However, our deembedding calibration-free technique, just as the GRL technique, requires application of proper gating process (specification of time span) to be discussed in Section III-B.

III. MEASUREMENT RESULTS

A. Experimental Setup and Specification of Time-Gating Span

The experimental setup used to validate our proposed free-space calibration-free technique is shown in Fig. 2. A VNA purchased from Keysight Technologies with model number N9918A was operated as the central unit of uncalibrated S-parameter measurements. This VNA has a frequency span from 30 kHz to 26.5 GHz, and a dynamic range around
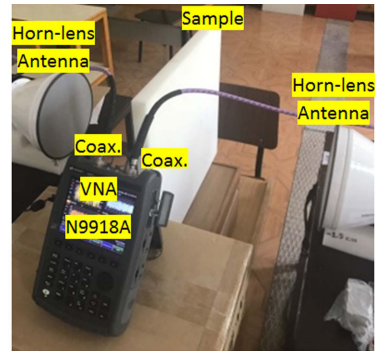

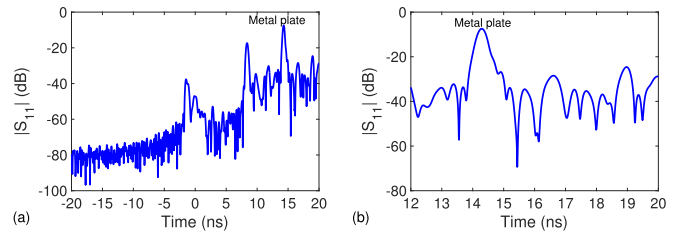Fig. 2. Photograph of the experimental setup used for validation of our method.

Fig. 3. Magnitudes of reflected signal $|S_{11}|$ in decibel over time when a highly reflective metal plate is positioned approximately at the midplane between two antennas. (a) View over a broader time span between -20 and 20 ns. (b) View over a narrower time span between 12 and 20 ns.

90 dB, and a directivity nor less than 32 dB entire frequency band. Two highly accurate stable coaxial cables with length 100 cm were connected between VNA ports and two coax-to-waveguide adapters to transfer electromagnetic signals from the VNA to two horn-lens antennas. These antennas purchased from Flann Microwave Instruments (Series 820) with maximum 1.5 VSWR value operating at X-band (8.2–12.4 GHz) were constructed to perform free-space measurements. The distance between sample front and rear faces apertures was set approximately 40 cm according to the antenna manual.

Prior to ε_r measurements of dielectric planar samples by our proposed technique, the time span for the application of time gating was specified. Toward this end, a highly reflective (no need to know its reflectivity value) metal plate with a transverse area of 50×50 cm^2 and a thickness of around 3 mm (the thickness value is not important) was positioned approximately at the midplane between the antennas (the distance between antennas was approximately 110 cm), and magnitude of reflection S-parameter $|S_{11}|$ was measured in time-domain while this plate was being moved. For example, Fig. 3(a) and (b) illustrates, respectively, the measured $|S_{11}|$ in decibel over broader (between -20 and 20 ns) and narrower (between 12 and 20 ns) time spans when this metal plate was positioned nearly at the midplane between the antennas. The reason of using 0 ns as the starting value of the time span and keeping the time span as large as possible (between -20 and 20 ns) was to conveniently detect the highest peak value of $|S_{11}|$ in time-domain which corresponds to the time value when the wavefront of electromagnetic signals impinged the front surface of the metal plate. For example, as seen from
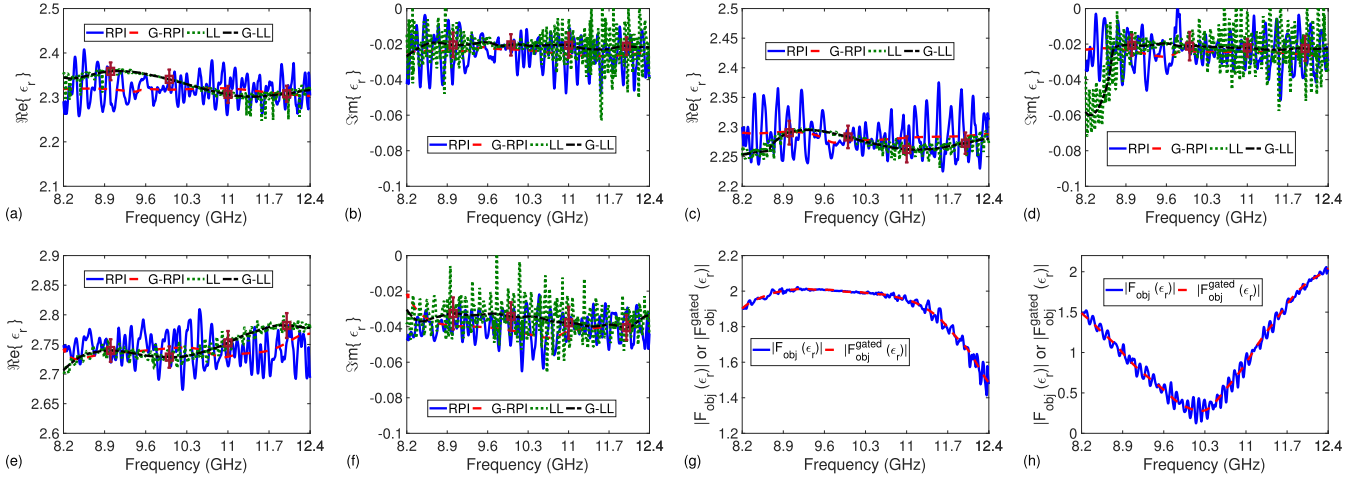
Fig. 4. Measured (a) real and (b) imaginary parts of ε_r of the PE sample, (c) real and (d) imaginary parts of ε_r of the PP sample, (e) real and (f) imaginary parts of ε_r of the POM sample, and magnitudes of $F_{\text{obj}}(\varepsilon_r)$ in (9) over frequency with/out gating process for (g) PE sample and (h) POM sample. Extraction methods are the calibration-dependent method in the study [45] after the TRL calibration procedure (denoted by "RPI"—blue solid line) and after the calibration procedure along with gating (denoted by "G-RPI"—red dashed line), the calibration-free deembedding method (denoted by "LL"—green dashdot line) using F_{obj} in (9) along with the application of the rolling average, and the proposed calibration-free deembedding method (denoted by "G-LL"—black dashed line) with gating using F_{obj} in (9). Error bars represented by violet color are calculated at $f = 9.0, 10.0, 11.0,$ and 12.0 GHz.

Fig. 3(a) and (b), this peak value is approximately $|S_{11}|_{\text{peak}} \cong -7.46$ dB occurring at $t_{\text{peak}} = 14.29$ ns. In order to ensure whether this peak value was arising from the metal plate, as a cross check, additional $|S_{11}|$ measurements in time-domain were conducted when the metal plate was moved to another distant location from the midplane between the antennas toward the horn-lens antenna to which the port-2 of the VNA was connected. From these measurements, it was noted that there was no noticeable change in the temporal response of $|S_{11}|$ before $t = 14.29$ ns, validating that the peak of $|S_{11}|_{\text{peak}} \cong -7.46$ dB occurring at $t_{\text{peak}} = 14.29$ ns was due to the metal plate used in our measurements.

B. Extracted Permittivity

Three different low-loss dielectric samples were utilized to validate our proposed method and examine its accuracy compared with the accuracy of other methods. These are the polyethylene (PE) sample with $L = 31.0 \mp 0.3$ mm, the polypropylene (PP) sample with $L = 30.3 \mp 0.3$ mm, and the polyoxymethylene (POM) sample with $L = 30.0 \mp 0.3$ mm. Each sample had approximately a transverse area of 50×50 cm^2 to eliminate the diffraction effects that could be observed at sample corners and edges. We did not use pyramidal microwave absorbers [16] in our experimental setup due to a sufficient degree of focusing capability of horn-lens antennas. S-parameter measurements were performed between 8.2 and 12.4 GHz with 1001 frequency points and were repeated independently (removal and reposition of each sample) five times for each sample for each applied method to reduce measurement errors and to compute standard deviations.

Fig. 4(a)–(f) illustrates retrieved real and imaginary parts of ε_r of PE, PP, and POM samples, respectively, by the proposed deembedding method (denoted by "G-line-line (LL)") using F_{obj} in (9) with time gating over the time period between $t_{\text{init}} = 13.790$ ns $(= t_{\text{peak}} - 500$ ps) and $t_{\text{final}} = 15.290$ ns

$(= t_{\text{peak}} + 1000$ ps) from averaged S-parameters. To examine how much time-gating feature eliminates the ripple in the extracted ε_r and thus improves the accuracy, we also applied the calibration-free deembedding method (denoted by "LL") using F_{obj} in (9) without gating, after the rolling average was applied for a frequency width of 42 MHz [38] to from averaged S-parameters. For both of these calibration-free methods, the "fminsearch" function of MATLAB was used (the tolerance value of 10^{-10} and maximum evaluations of 10^5) with the initial values for each sample provided from $\varepsilon \cong 2.36(1 - j0.00069)$ at 9.5 GHz for the PE sample [47], $\varepsilon_r \cong 2.26(1 - j0.00008)$ at 9.4 GHz for the PP sample [46], and $\varepsilon_r \cong 2.73(1 - j0.00513)$ at approximately 11 GHz for the POM sample [46].

Besides, the calibration-dependent method in the study [45] was also employed to compare the accuracy of our proposed method. Before its application, the TRL calibration technique [26] and the GRL calibration technique [43], [44] were separately implemented. For the line standard, an air section of approximately 7.281 mm in length (quarter wavelength corresponding to the mid-frequency 10.3 GHz) was utilized for both calibration techniques. The metal plate with high reflectivity (not need to be known) and a transverse area of 50×50 cm^2, which is the same metal plate we used in finding time location for application of time gating by our method, was operated as the reflect standard for both calibration techniques. The extracted ε_r values by the calibration-dependent method in the study [45] using from averaged S-parameters are presented by the "reference-plane-invariant (RPI)" and "G-RPI" abbreviations in Fig. 4(a)–(f) depending on the calibration techniques TRL and GRL, respectively. In implementation of the calibration-dependent method in the study [45], the stepwise technique [48] was applied to extract unique solution for ε_r.

The following points are noted from the extracted ε_r of PE, PP, and POM samples in Fig. 4(a)–(f). First, real and imaginary

parts of ε_r values of PE, PP, and POM samples retrieved by all applied extraction methods are in good agreement with their reference values [46], [47]. Second, ε_r values retrieved by the calibration-dependent method in the study [45] after the TRL calibration technique ("RPI") and the calibration-free deembedding technique ("LL") produce some ripples over the full frequency band. Such ripples are mainly due to multiple reflections between antennas and sample faces (due to impedance mismatch between antenna and air) and undesired reflection from ground. These ripples are greatly mitigated from extracted ε_r by the gating process as seen from the results presented by "G-RPI" and "G-LL" in Fig. 4(a)–(f). Third, extracted imaginary parts of ε_r by the calibration-dependent method in the study [45] (without gating) and by the calibration-free deembedding technique (without gating) at some frequencies violate the passivity principle which states that $\Im\{\varepsilon_r\} \leq 0$ for the time reference in the form $\exp(+j\omega t)$ where $\Im\{\star\}$ denotes the imaginary part of "$\star$." For example, while $\Im m\{\varepsilon_r\}$ of the PP sample extracted by the calibration-dependent method in the study [45] (without gating) is 0.056 at 9.792 GHz, that extracted by the calibration-free deembedding technique (without gating) is 0.012 at 12.22 GHz. Fourth, standard deviations calculated from five independent measurements are less than approximately 4% and 10% for the real and imaginary parts of ε_r for each sample, respectively. This shows the integrity of the measured ε_r by the proposed method. Fifth, as compared with the reference data in [46] and [47], relatively higher extracted $\Im m\{\varepsilon_r\}$ values by our method and the method in [45] with or without gating could be attributed to the limited accuracy of nonresonant techniques in the extraction $\Im m\{\varepsilon_r\}$ in low-loss samples.

We also performed some further analysis to examine the effect of time-gating in the extraction process by our method. In this regard, magnitude of $F_{obj}(\varepsilon_r)$ in (9) with/out time-gating was evaluated for each sample. For example, Fig. 4(g) and (h) illustrates the frequency dependence of the magnitude of $F_{obj}(\varepsilon_r)$ in (9) with/out time-gating for the PE and POM samples. Such a dependence for the PP sample is not demonstrated for simplicity. It is seen from the results in Fig. 4(g) and (h) that the magnitude of $F_{obj}(\varepsilon_r)$ with time-gating has a smoother frequency dependence than the magnitude of $F_{obj}(\varepsilon_r)$ without time-gating. This obviously explains much smoother dependence of extracted ε_r by the new deembedding technique as compared with that by the conventional one. On the other hand, we also evaluated the position-insensitive feature of the proposed method. To validate this feature, additional S-parameter measurements were carried out to retrieve ε_r of the PE sample by our method. Fig. 5(a) and (b) illustrates, respectively, the real and imaginary parts and their relative changes of ε_r of the PE sample by the proposed method using the $F_{obj}(\varepsilon_r)$ in (9) after applying time-gating over the time period between $t_{init} = 13.790$ ns ($= t_{peak} - 500$ ps) and $t_{final} = 15.290$ ns ($= t_{peak} + 1000$ ps) from averaged S-parameters when the sample was moved 5 cm toward the receiving antenna in Fig. 1. It is seen from Fig. 5(a) and (b) that extracted ε_r values of the PE sample by the proposed method, when the sample was at the midplane and 5 cm away from the midplane, are very close to one another
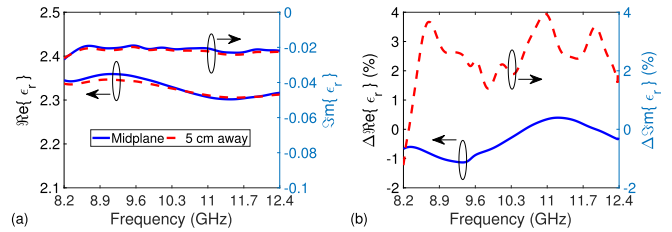

Fig. 5. (a) Measured real and imaginary parts of ε_r and (b) their relative changes of the PE sample by the proposed calibration-free deembedding method with gating using F_{obj} in (9) when the sample was at the midplane and 5 cm away from the midplane.

(less than 1% and 4% changes for the real and imaginary parts over the full frequency band). Relatively higher change in $\Im m\{\varepsilon_r\}$ as compared with $\Re e\{\varepsilon_r\}$ for a change in the position of the sample from the midplane could be attributed to low-loss nature of the PE sample. These results validate that our proposed method is not sensitive to (or changing comparatively smaller with) the position of the sample.

Finally, it is instructive to discuss the limitations of our method. First, its accuracy decreases if the incident wave on the surface of the sample is not a plane wave due to converging/diverging waves (e.g., the beam waist should be a plane wavefront) because the whole theory is based on this assumption. It means that the sample should be positioned near (but not exactly at) the midplane between antennas. Second, not only the sample surface should be planar (or surface roughness should be small compared with the wavelength [18]) but also it should be parallel to the antenna aperture (tilt angle should be either zero or small [16]). Third, our method is only limited to homogeneous and isotropic samples. Finally, the accuracy of our method decreases for extremely low-loss samples at Fabry–Perot frequencies [20] due to increased uncertainty in measured S_{11} and/or S_{22} and for lossy samples producing at least -40 dB attenuation due to increased uncertainty in measured S_{21} and/or S_{12}. In addition, inaccurate information of the sample thickness also limits the accuracy of our proposed method.

IV. CONCLUSION

We proposed a new deembedding calibration-free technique for accurate ε_r measurement of flat dielectric samples using free-space measurements. Accuracy, ripple-free property, calibration-free flexibility, and position-insensitivity are the key features of our proposed method. Measurement configurations of the conventional calibration-free deembedding method and the proposed calibration-free deembedding method are first presented and next the objective functions for both methods are derived using the WCM formulation and its similarity feature (trace operation). Then, the time span for time gating process in implementation of our method is evaluated by moving a metal plate around the midplane of transmitting and receiving antennas and recording the height peak value of $|S_{11}|$ in the time-domain. After our method is applied for extracting ε_r of the PE, PP, and POM dielectric samples using the derived objective function using 2-D "fminsearch" function

of MATLAB, and the accuracy of our method is also compared with the accuracy of other calibration-free and calibration-dependent methods. From this comparison, it is noted that our proposed method extracts accurate ε_r values (in parallel with the passivity principle and in agreement with the reference values in the literature), while two of the tested methods retrieve nonphysical ε_r including some ripples (violation of the passivity principle) at some frequencies. Position-insensitivity of our method was also validated by measurements away from the midplane of the antennas. The proposed method can find applications for health monitoring of specimens (delamination analysis and detection of defects such as faults and anomalies) in industry.

REFERENCES

[1] L. F. Chen, C. K. Ong, C. P. Neo, V. V. Varadan, and V. K. Varadan, *Microwave Electronics: Measurement and Materials Characterization.* West Sussex, U.K.: Wiley, 2004.

[2] Z. J. Wong *et al.*, "Optical and acoustic metamaterials: Superlens, negative refractive index and invisibility cloak," *J. Opt.*, vol. 19, no. 8, Jul. 2017, Art. no. 084007.

[3] F. Han, L. Yin, C. Du, and P. Liu, "Robust effective-medium characteristics of bianisotropic reflective metasurfaces based on field-circuit combined analysis," *Adv. Theory Simul.*, vol. 4, no. 2, Feb. 2021, Art. no. 2000246.

[4] Q.-Q. Ni, J. Hong, P. Xu, Z. Xu, K. Khvostunkov, and H. Xia, "Damage detection of CFRP composites by electromagnetic wave nondestructive testing (EMW-NDT)," *Compos. Sci. Technol.*, vol. 210, Jul. 2021, Art. no. 108839.

[5] H. Hasar *et al.*, "Prediction of water-adulteration within honey by airline de-embedding waveguide measurements," *Measurement*, vol. 179, Jul. 2021, Art. no. 109469.

[6] J. Krupka, "Frequency domain complex permittivity measurements at microwave frequencies," *Meas. Sci. Technol.*, vol. 17, no. 6, pp. R55–R70, Apr. 2006.

[7] J. Sheen, "Comparisons of microwave dielectric property measurements by transmission/reflection techniques and resonance techniques," *Meas. Sci. Technol.*, vol. 20, no. 4, Jan. 2009, Art. no. 042001.

[8] A. M. Nicolson and G. F. Ross, "Measurement of the intrinsic properties of materials by time-domain techniques," *IEEE Trans. Instrum. Meas.*, vol. IT-19, no. 4, pp. 377–382, Nov. 1970.

[9] D. K. Ghodgaonkar, V. V. Varadan, and V. K. Varadan, "Free-space measurement of complex permittivity and complex permeability of magnetic materials at microwave frequencies," *IEEE Trans. Instrum. Meas.*, vol. 39, no. 2, pp. 387–394, Apr. 1990.

[10] X. Liu, L. Gan, and B. Yang, "Millimeter-wave free-space dielectric characterization," *Measurement*, vol. 179, Jul. 2021, Art. no. 109472.

[11] V. V. Varadan, R. D. Hollinger, D. K. Ghodgaonkar, and V. K. Varadan, "Free-space, broadband measurements of high-temperature, complex dielectric properties at microwave frequencies," *IEEE Trans. Instrum. Meas.*, vol. 40, no. 5, pp. 842–846, Oct. 1991.

[12] J. Frolik, "Reconstruction of multilayered lossy dielectrics from one-sided plane wave impulse reflection responses: The bistatic case," *IEEE Trans. Geosci. Remote Sens.*, vol. 39, no. 9, pp. 2051–2059, Sep. 2001.

[13] S. Caorsi and M. Stasolla, "A layer stripping approach for EM reconstruction of stratified media," *IEEE Trans. Geosci. Remote Sens.*, vol. 52, no. 9, pp. 5855–5869, Sep. 2014.

[14] I. Vakili, L. Ohlsson, L.-E. Wernersson, and M. Gustafsson, "Time-domain system for millimeter-wave material characterization," *IEEE Trans. Microw. Theory Techn.*, vol. 63, no. 9, pp. 2915–2922, Sep. 2015.

[15] Z. Akhter and M. J. Akhtar, "Free-space time domain position insensitive technique for simultaneous measurement of complex permittivity and thickness of lossy dielectric samples," *IEEE Trans. Instrum. Meas.*, vol. 65, no. 10, pp. 2394–2405, Oct. 2016.

[16] U. C. Hasar *et al.*, "Complex permittivity and thickness evaluation of low-loss dielectrics from uncalibrated free-space time-domain measurements," *IEEE Trans. Geosci. Remote Sens.*, vol. 60, pp. 1–10, 2022.

[17] K.-I. Murata, A. Hanawa, and R. Nozaki, "Broadband complex permittivity measurement techniques of materials with thin configuration at microwave frequencies," *J. Appl. Phys.*, vol. 98, no. 8, Oct. 2005, Art. no. 084107.

[18] S. N. Kharkovsky, M. F. Akay, U. C. Hasar, and C. D. Atis, "Measurement and monitoring of microwave reflection and transmission properties of cement-based specimens," *IEEE Trans. Instrum. Meas.*, vol. 51, no. 6, pp. 1210–1218, Dec. 2002.

[19] J. Hammler, A. J. Gallant, and C. Balocco, "Free-space permittivity measurement at terahertz frequencies with a vector network analyzer," *IEEE Trans. THz Sci. Technol.*, vol. 6, no. 6, pp. 817–823, Nov. 2016.

[20] S. Kim, D. Novotny, J. Gordon, and J. Guerrieri, "A free-space measurement method for the low-loss dielectric characterization without prior need for sample thickness data," *IEEE Trans. Antennas Propag.*, vol. 64, no. 9, pp. 3869–3879, Sep. 2016.

[21] C. Yang, K. Ma, and J.-G. Ma, "A noniterative and efficient technique to extract complex permittivity of low-loss dielectric materials at terahertz frequencies," *IEEE Antennas Wireless Propag. Lett.*, vol. 18, no. 10, pp. 1971–1975, Oct. 2019.

[22] C. A. Grosvenor, R. T. Johnk, J. Baker-Jarvis, M. D. Janezic, and B. Riddle, "Time-domain free-field measurements of the relative permittivity of building materials," *IEEE Trans. Instrum. Meas.*, vol. 58, no. 7, pp. 2275–2282, Jul. 2009.

[23] A. Rashidian, L. Shafai, D. Klymyshyn, and C. Shafai, "A fast and efficient free-space dielectric measurement technique at mm-wave frequencies," *IEEE Antennas Wireless Propag. Lett.*, vol. 16, pp. 2630–2633, 2017.

[24] L. Li, H. Hu, P. Tang, R. Li, B. Chen, and Z. He, "Compact dielectric constant characterization of low-loss thin dielectric slabs with microwave reflection measurement," *IEEE Antennas Wireless Propag. Lett.*, vol. 17, no. 4, pp. 575–578, Apr. 2018.

[25] U. C. Hasar, "Non-destructive testing of hardened cement specimens at microwave frequencies using a simple free-space method," *NDT E Int.*, vol. 42, no. 6, pp. 550–557, Sep. 2009.

[26] G. F. Engen and C. A. Hoer, "Thru-reflect-line: An improved technique for calibrationg the dual 6-port automatic network analyzer," *IEEE Trans. Microw. Theory Techn.*, vol. MTT-27, no. 12, pp. 983–987, Dec. 1979.

[27] H.-J. Eul and B. Schiek, "A generalized theory and new calibration procedures for network analyzer self-calibration," *IEEE Trans. Microw. Theory Techn.*, vol. 39, no. 4, pp. 724–731, Apr. 1991.

[28] I. Rolfes and B. Schiek, "Calibration methods for microwave free space measurement," *Adv. Radio Sci.*, vol. 2, pp. 19–25, May 2004.

[29] T. Ozturk, M. Hudlička, and I. Uluer, "Development of measurement and extraction technique of complex permittivity using transmission parameter s 21 for millimeter wave frequencies," *J. Infr., Millim., THz Waves*, vol. 38, no. 12, pp. 1510–1520, Dec. 2017.

[30] C. Wan, B. Nauwelaers, W. De Raedt, and M. Van Rossum, "Two new measurement methods for explicit determination of complex permittivity," *IEEE Trans. Microw. Theory Techn.*, vol. 46, no. 11, pp. 1614–1619, Nov. 1998.

[31] M. D. Janezic and J. A. Jargon, "Complex permittivity determination from propagation constant measurements," *IEEE Microw. Guided Wave Lett.*, vol. 9, no. 2, pp. 76–78, Feb. 1999.

[32] J. A. Reynoso-Hernandez, C. F. Estrada-Maldonado, T. Parra, K. Grenier, and J. Graffeuil, "An improved method for the wave propagation constant? Estimation in broadband uniform millimeter-wave transmission line," *Microw. Opt. Technol. Lett.*, vol. 22, no. 4, pp. 268–271, Aug. 1999.

[33] I. Huygen, C. Steukers, and F. Duhamel, "A wideband line-line dielectrometric method for liquids, soils, and planar substrates," *IEEE Trans. Instrum. Meas.*, vol. 50, no. 5, pp. 1343–1348, Oct. 2001.

[34] L. Lanzi, M. Carlà, C. M. C. Gambi, and L. Lanzi, "Differential and double-differential dielectric spectroscopy to measure complex permittivity in transmission lines," *Rev. Sci. Instrum.*, vol. 73, no. 8, pp. 3085–3088, Aug. 2002.

[35] U. C. Hasar, "Calibration-independent method for complex permittivity determination of liquid and granular materials," *Electron. Lett.*, vol. 44, no. 9, pp. 585–586, Apr. 2008.

[36] N. J. Farcich, J. Salonen, and P. M. Asbeck, "Single-length method used to determine the dielectric constant of polydimethylsiloxane," *IEEE Trans. Microw. Theory Techn.*, vol. 56, no. 12, pp. 2963–2971, Dec. 2008.

[37] Z. Caijun, J. Quanxing, and J. Shenhui, "Calibration-independent and position-insensitive transmission/reflection method for permittivity measurement with one sample in coaxial line," *IEEE Trans. Electromagn. Compat.*, vol. 53, no. 3, pp. 684–689, Aug. 2011.

[38] N. Jebbor, S. Bri, A. M. Sánchez, and M. Chaibi, "A fast calibration-independent method for complex permittivity determination at microwave frequencies," *Measurement*, vol. 46, no. 7, pp. 2206–2209, 2013.

[39] C. Guoxin, "Calibration-independent measurement of complex permittivity of liquids using a coaxial transmission line," *Rev. Sci. Instrum.*, vol. 86, no. 1, Jan. 2015, Art. no. 014704.

[40] U. C. Hasar, "Thickness-invariant complex permittivity retrieval from calibration-independent measurements," *IEEE Microw. Wireless Compon. Lett.*, vol. 27, no. 2, pp. 201–203, Feb. 2017.

[41] U. C. Hasar, "Self-calibrating transmission-reflection technique for constitutive parameters retrieval of materials," *IEEE Trans. Microw. Theory Techn.*, vol. 66, no. 2, pp. 1081–1089, Feb. 2018.

[42] D. Rytting, "Network analyzer error models and calibration methods," in *Proc. 62nd ARFTG Conf. Short Course. Notes*, Dec. 2003, pp. 1–43.

[43] P. G. Bartley and S. B. Begley, "Improved free-space S-parameter calibration," in *Proc. IEEE Instrumentationand Meas. Technol. Conf.*, May 2005, pp. 372–375.

[44] P. G. Bartley and S. B. Begley, "A new free-space calibration technique for materials measurement," in *Proc. IEEE Int. Instrum. Meas. Technol. Conf. Proc.*, May 2012, pp. 47–51.

[45] K. Chalapat, K. Sarvala, J. Li, and G. S. Paraoanu, "Wideband reference-plane invariant method for measuring electromagnetic parameters of materials," *IEEE Trans. Microw. Theory Techn.*, vol. 57, no. 9, pp. 2257–2267, Sep. 2009.

[46] B. Riddle, J. Baker-Jarvis, and J. Krupka, "Complex permittivity measurements of common plastics over variable temperatures," *IEEE Trans. Microw. Theory Techn.*, vol. 51, no. 3, pp. 727–733, Mar. 2003.

[47] A. K. Jha and M. J. Akhtar, "A generalized rectangular cavity approach for determination of complex permittivity of materials," *IEEE Trans. Instrum. Meas.*, vol. 63, no. 11, pp. 2632–2641, Nov. 2014.

[48] U. C. Hasar, J. J. Barroso, C. Sabah, Y. Kaya, and M. Ertugrul, "Stepwise technique for accurate and unique retrieval of electromagnetic properties of bianisotropic metamaterials," *J. Opt. Soc. Amer. B, Opt. Phys.*, vol. 30, no. 4, pp. 1058–1068, Apr. 2013.

Ugur Cem Hasar (Member, IEEE) received the B.Sc. and M.Sc. degrees (Hons.) in electrical and electronics engineering from Cukurova University, Adana, Turkey, in 2000 and 2002, respectively, and the Ph.D. degree (Hons.) in electrical and computer engineering from State University of New York at Binghamton, Binghamton, NY, USA, in 2008.

From 2000 to 2005, he was a Research and Teaching Assistant with the Department of Electrical and Electronics Engineering, Cukurova University. From 2005 to 2008, he was a Research Assistant with the Department of Electrical and Electronics Engineering, Ataturk University, Erzurum, Turkey. From 2009 to 2011 and from 2011 to 2013, he was an Assistant Professor and an Associate Professor with Ataturk University. Since 2017, he has been a Full-Time Professor with the Department of Electrical and Electronics Engineering, Gaziantep University, Gaziantep, Turkey. His main research interests include nondestructive testing and evaluation of materials using microwaves, novel calibration-dependent, calibration-independent techniques for the electrical and physical characterization of conventional materials at microwaves, millimeter waves, and terahertz frequencies, high-temperature packaging for high power density applications, porous silicon-based devices and their applications, and metamaterials.

Prof. Hasar was a recipient of the Outstanding Young Scientist Award in Electromagnetics of Leopold B. Felsen Fund, the Binghamton University Distinguished Dissertation Award, the Binghamton University Graduate Student Award for Excellence in Research, and the Science Academy's Young Scientist Award.

Yunus Kaya received the B.Sc. degree in electrical and electronics engineering, the B.Sc. degree in mechanical engineering, and the M.Sc. and Ph.D. degrees in electrical and electronics engineering from Atatürk University, Erzurum, Turkey, in 2011, 2013, 2013, and 2020, respectively.

Since 2020, he has been an Assistant Professor with the Department of Electricity and Energy, Bayburt University, Bayburt, Turkey. His research area involves the characterization of materials by microwaves and metamaterials.

Hamdullah Ozturk received the B.Sc. degree from the Department of Electrical and Electronics Engineering, University of Atılım, Ankara, Turkey, in 2015, and the M.Sc. degree from the Department of Electrical and Electronics Engineering, Iskenderun Technical University, İskenderun, Turkey, in 2018. He is currently pursuing the Ph.D. degree with the Department of Electrical and Electronics Engineering, Gaziantep University, Gaziantep, Turkey.

His current research interests include the characterization of materials by microwave sensors and antenna.

Mucahit Izginli received the B.Sc. degree from the Department of Electrical and Electronics Engineering, Gaziantep University, Gaziantep, Turkey, in 2018, where he is currently pursuing the M.Sc. degree.

Since 2020, he has been working as a Research Assistant with the Department of Electrical and Electronics Engineering, Hasan Kalyoncu University, Gaziantep. His current research interests include the characterization of materials by microwave sensors and antenna.

Mehmet Ertugrul (Member, IEEE) received the B.Sc. degree from the Department of Physics, Atatürk University, Erzurum, Turkey, in 1986, and the M.Sc. and Ph.D. degrees in atomic physics from Atatürk University, in 1990 and 1994, respectively.

From 1994 to 1996, from 1996 to 2001, and from 2001 to 2002, he was an Assistant Professor, an Associate Professor, and a Full Professor with the Department of Physics, Atatürk University, respectively, where he has been a Full Professor with the Department of Electrical and Electronics Engineering, since 2003. He has authored or coauthored more than 120 articles published in international journals. His current research interests include superconducting and semiconducting devices with applications, nanofabrication, and nanoelectronics.

Prof. Ertugrul was a recipient of the Award by The Scientific and Technological Research Council of Turkey and the Turkish Academy of Sciences.

Joaquim José Barroso (Member, IEEE) received the B.Sc. degree in electronics engineering and the M.Sc. degree in plasma physics from the Instituto Tecnológico de Aeronáutica, São José dos Campos, Brazil, in 1976 and 1980, respectively, and the Ph.D. degree in plasma physics from the INPE-Instituto Nacional de Pesquisas Espaciais, São José dos Campos, in 1988.

From 1989 to 1990, he was a Visiting Scientist with the Massachusetts Institute of Technology, Cambridge, MA, USA. Since 1982, he has been with the INPE-Instituto Nacional de Pesquisas Espaciais, where he was involved in the design and construction of high-power microwave tubes. His current research interests include microwave electronics, plasma technology, electromagnetics, and metamaterials.

Omar M. Ramahi (Fellow, IEEE) was born in Jerusalem, Palestine. He received the two B.S. degrees (Hons.) in mathematics and electrical and computer engineering from Oregon State University, Corvallis, OR, USA, in 1984, and the Ph.D. degree in electrical and computer engineering from the University of Illinois at Urbana-Champaign (UIUC), Champaign, IL, USA, in 1990.

He then worked with Digital Equipment Corporation (presently, HP), Maynard, MA, USA, where he was a Member of the Alpha Server Product Development Group. In 2000, he joined as a Faculty of the James Clark School of Engineering, University of Maryland, College Park, MD, USA, as an Assistant Professor and later as a tenured Associate Professor. At Maryland, he was also a Faculty Member of the CALCE Electronic Products and Systems Center. He is currently a Professor with the Electrical and Computer Engineering Department, University of Waterloo, Waterloo, ON, Canada. He has authored and coauthored more than 450 journal articles and conference technical papers on topics related to the electromagnetic phenomena and computational techniques to understand the same. He is the coauthor of the book *EMI/EMC Computational Modeling Handbook*.

Prof. Ramahi was a winner of the 2004 University of Maryland Pi Tau Sigma Purple Cam Shaft Award. He was a recipient of the Excellent Paper Award in the 2004 International Symposium on Electromagnetic Compatibility, Sendai, Japan, and the 2010 University of Waterloo Award for Excellence in Graduate Supervision. In 2012, he was awarded the IEEE Electromagnetic Compatibility Society Technical Achievement Award.